Mechanics of Composite Materials, Vol. 45, No. 6, 2009

CALCULATION OF COMPOSITE STRUCTURES SUBJECTED TO FOLLOWER LOADS BY USING A GEOMETRICALLY EXACT SHELL ELEMENT

G. M. Kulikov and S. V. Plotnikova

Keywords: *multilayer composite shell, follower load, geometrically exact shell element, 7-parameter shell model*

Based on a 7-parameter shell model, a numerical algorithm has been developed for solving the geometrically nonlinear problem of a multilayer composite shell subjected to a follower pressure and undergoing large displacements and rotations. As unknowns, six displacements of the outer surfaces and additionally the transverse displacement of midsurface of the shell are chosen. This allows one to use the Green–Lagrange strain tensor, introduced earlier by the authors, which exactly represents arbitrarily large rigid-body displacements of the shell in curvilinear coordinates of a reference surface. A geometrically exact solid shell element is formulated, which permits one to solve the nonlinear deformation problem for thin-walled composite structures subjected to a follower pressure by using a very small number of load steps.

Introduction

During the last years, a great deal of attention has been focused on the development of isoparametric three-dimensional finite shell elements, which give satisfactory results in solving the geometrically nonlinear mechanical problems of thin-walled composite structures subjected to follower loads [1-3]. Their particular feature is that the initial and deformed configurations of the shell are interpolated uniformly in a global Cartesian system of coordinates, and thus great rigid-body displacements can be described correctly. However, the isoparametric shell element is computationally inefficient in calculating composite structures loaded with a follower pressure and subjected to arbitrarily large rotations, since it requires a rather great number of loading steps.

An alternative is the geometrically exact finite shell elements based on the nonlinear deformation relations of 6- and 7-parametric 3D shell models introduced in [4-9], which exactly represent arbitrarily large rigid-body displacements in curvilinear coordinates of a reference surface. The term *geometrically exact* means that the reference surface of the shell is described by functions assigned analytically, in particular, by splines [10-12], which make the basis of modern CAD systems. In this case, the vectors of displacements of external and middle surfaces are represented in a local basis related to the reference surface of the shell. This factor allows one to decrease the number of loading steps considerably.

Tambov State Technical University, Russia. Translated from Mekhanika Kompozitnykh Materialov, Vol. 45, No. 6, pp. 789-804, November-December, 2009. Original article submitted January 20, 2009.

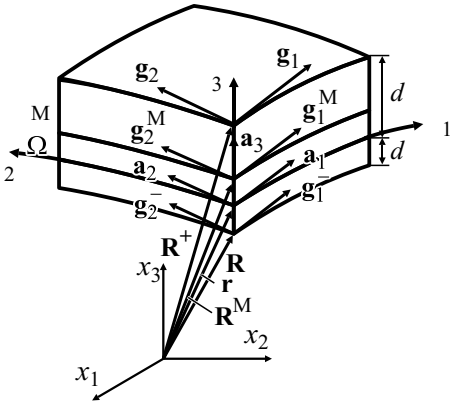

Fig. 1. Geometry of a shell.

In the present study, a more general geometrically exact 7-parameter bilinear shell element is presented for calculating thin-walled multilayer composite structures under the action of follower loads. To struggle against the emergence of both the shear and the membrane lockings known in the finite-element method (FEM), a hybrid FEM model was used. According to this model, the strains and resulting displacements inside the shell element are approximated independently. We should note that the 6-parameter model [4-8], postulating a uniform distribution of the transverse normal strains across the thickness of layer package, often leads to the Poisson locking of shell elements, while the 7-parameter model is free from this drawback [9, 13, 14].

7-Parameter Model of a Composite Shell

Let us consider a thin shell of thickness h d d consisting of NL elastic anisotropic layers of constant thickness h_k. We assume that, at each point of the shell, there exists a surface of elastic symmetry parallel to a reference surface . As the reference surface, we consider an inner surface of some k-layer or an interface between layers and relate it to curvilinear orthogonal coordinates $_1$ and $_2$, reckoned along the lines of main curvatures. The transverse coordinate $_3$ is reckoned toward the increasing external normal to the surface (Fig. 1). Let $\mathbf{e}_1$ and $\mathbf{e}_2$ be the unit vectors of tangents to the coordinate lines $_1$ and $_2$, $\mathbf{a}_3$ $\mathbf{e}_3$ the unit vector of the external normal, A Lamé parameters, k the main curvatures, d^{A} the distances from the reference to external surfaces $^{\mathrm{A}}$, $\mathbf{r}(\ _1,\ _2)$ the radius vector of the reference surface , $\mathbf{R}^{\mathrm{M}}(\ _1,\ _2)$ the radius vector of the midsurface $^{\mathrm{M}}$, and $\mathbf{R}^{\mathrm{A}}(\ _1,\ _2)$ the radii vectores of the external surfaces $^{\mathrm{A}}$. Hereinafter, $= 1, 2,..., NL$; , $= 1, 2$; $i, j, l, m = 1, 2, 3$; A , .

For the radii vectores of the middle and external surfaces of the shell, we have

$$\mathbf{R}^{I} \quad \mathbf{r} \quad z^{I}\mathbf{a}_3 \quad (I \quad ,\mathrm{M},\ ), \qquad (1)$$

$$z \quad d\ , \quad z \quad d\ , \quad z^{\mathrm{M}} \quad \frac{1}{2}(z \quad z\ ).$$

wherefrom follow the formulas for base vectors (see Fig. 1)

$$\mathbf{a} \quad \mathbf{r}_{,} \quad A\ \mathbf{e}\ , \quad \mathbf{g}^{I} \quad \mathbf{R}^{I}_{,} \quad A\ c^{I}\mathbf{e}\ , \qquad (2)$$

$$c^I \quad 1 \quad k \quad z^I \quad (I \quad ,\mathrm{M}, \quad).$$

Let us assume that the tangential and transverse displacements are distributed across the shell thickness according to the linear and square laws, respectively [15], i.e.,

$$u \quad \underset{\mathrm{A}}{N^{\mathrm{A}} u^{\mathrm{A}}}, \quad u_3 \quad \underset{I}{L^I u_3^I} \quad (I \quad ,\mathrm{M}, \quad), \tag{3}$$

where $u^{\mathrm{A}}(\ _1, \ _2)$ and $u_3^{\mathrm{A}}(\ _1, \ _2)$ are the tangential and transverse displacements of the external surfaces; $u_3^{\mathrm{M}}(\ _1, \ _2)$ is the transverse displacement of the midsurface; $N^{\mathrm{A}}(\ _3)$ and $L^I(\ _3)$ are the Lagrange polynomials of the first and second degrees, respectively:

$$N \quad \frac{1}{h}(z \quad _3), \quad N \quad \frac{1}{h}(\ _3 \quad z \quad),$$
$$L \quad N \quad (N \quad N \quad), \quad L^{\mathrm{M}} \quad 4N \quad N \quad , \quad L^{+} \quad N \quad (N \quad N \quad). \tag{4}$$

In this case, $L^I(z^J) = 1$ if $J \quad I$, and $L^I(z^J) = 0$ if $J \quad I$.

Introducing displacements (3), with account of Eqs. (4), into the deformation relations of the three-dimensional elasticity theory and assuming that all components (except for the transverse tangential ones) of the Green–Lagrange strain tensor vary linearly across the thickness of the layer package [9], we come to the strain relations of the 7-parameter shell model

$$\underset{\mathrm{A}}{N^{\mathrm{A}} \ ^{\mathrm{A}}} \ , \quad _{33} \quad \underset{\mathrm{A}}{N^{\mathrm{A}} \ ^{\mathrm{A}}_{33}},$$
$$_3 \quad \widehat{\ } \ _3, \quad \widehat{\ } \ _3 \quad \frac{1}{2}(\ _3 \quad \ _3). \tag{5}$$

Here, $_{ij}(\ _1, \ _2)$ are the strains of external surfaces of the shell, which are determined by the formulas

$$2 \ ^{\mathrm{A}} \quad c^{\mathrm{A}} \ ^{\mathrm{A}} \quad c^{\mathrm{A}} \ ^{\mathrm{A}} \quad \underset{i}{^{\mathrm{A}}_{i}} \ ^{\mathrm{A}}_{i} \ , \quad 2 \ ^{\mathrm{A}}_{3} \quad c^{\mathrm{A}} \ ^{\mathrm{A}} \quad ^{\mathrm{A}}_{3} \quad \underset{i}{^{\mathrm{A}}_{i}} \ ^{\mathrm{A}}_{i} \ ,$$
$$2 \ ^{\mathrm{A}}_{3} \quad 2 \ ^{\mathrm{A}}_{3} \quad \underset{i}{^{\mathrm{A}}_{i}} \ ^{\mathrm{A}}_{i}, \tag{6}$$

where

$$^{\mathrm{A}} \quad \frac{1}{A} u^{\mathrm{A}} \quad \underset{,}{B \quad u^{\mathrm{A}} \quad B \quad u^{\mathrm{A}} \quad k \quad u_3^{\mathrm{A}}} \quad (\quad),$$
$$^{\mathrm{A}} \quad \frac{1}{A} u^{\mathrm{A}} \quad \underset{,}{B \quad u^{\mathrm{A}} \quad B \quad u^{\mathrm{A}}} \quad (\quad), \tag{7}$$
$$^{\mathrm{A}}_{3} \quad \frac{1}{A} u_3^{\mathrm{A}} \quad \underset{,}{B \quad u_3^{\mathrm{A}} \quad k \quad u^{\mathrm{A}}, \quad B \quad \frac{1}{A \ A} A} \ , \ ,$$

$$_i \quad \frac{1}{h}(\ 3u_i \quad 4u_i^{\mathrm{M}} \quad u_i\ ), \quad _i \quad \frac{1}{h}(u_i \quad 4u_i^{\mathrm{M}} \quad 3u_i\ ), \ u^{\mathrm{M}} \quad \frac{1}{2}(u \quad u\ ).$$

Deformation relations (5)-(7) are rather attractive from the viewpoint of their use in the FEM, since they *exactly* represent arbitrarily large rigid-body displacements [9]. Another advantage of these strain relations is that they allow one to overcome the so-called Poisson locking (artificial overestimation of shell rigidity in the transverse direction) [14].

The radii vectores of external surfaces of the deformed shell can be presented in the form

$$\overline{\mathbf{R}}^{\mathrm{A}} \quad \mathbf{R}^{\mathrm{A}} \quad \mathbf{u}^{\mathrm{A}}, \tag{8}$$

$$\mathbf{u}^{\mathrm{A}} \quad \underset{i}{} \ u_i^{\mathrm{A}}\mathbf{e}_i . \tag{9}$$

Differentiating equalities (8) and (9) and taking into account Eq. (2), we come to the expressions for the base vectors of external surfaces of the deformed shell

$$\overline{\mathbf{g}}^{\mathrm{A}} \quad \overline{\mathbf{R}}_{,}^{\mathrm{A}} \quad \mathbf{g}^{\mathrm{A}} \quad \mathbf{u}^{\mathrm{A}}, \tag{10}$$

wherefrom follows the formula for the unit vector of the normal to the external surface of the deformed shell

$$\mathbf{n}^{\mathrm{A}} \quad \frac{1}{\left|\overline{\mathbf{g}}_1^{\mathrm{A}} \quad \overline{\mathbf{g}}_2^{\mathrm{A}}\right|}\overline{\mathbf{g}}_1^{\mathrm{A}} \quad \overline{\mathbf{g}}_2^{\mathrm{A}}. \tag{11}$$

Taking into account the known formulas of differentiation of the base vectors $\mathbf{e}_i$ with respect to the coordinates [16] and the representations for displacement vectors (9), we have

$$\mathbf{u}_{,}^{\mathrm{A}} \quad A \quad \underset{i}{} \ {}_i^{\mathrm{A}}\ \mathbf{e}_i . \tag{12}$$

Using relations (2) and (10)-(12), we arrive at the sought-for formula for the normal vector

$$\mathbf{n}^{\mathrm{A}} \quad \frac{1}{\mathrm{A}} \quad \underset{i}{} \ {}_i^{\mathrm{A}}\mathbf{e}_i, \tag{13}$$

$$\begin{gathered} {}_1^{\mathrm{A}} \quad {}_{21}^{\mathrm{A}}\ {}_{32}^{\mathrm{A}} \quad {}_{31}^{\mathrm{A}}(c_2^{\mathrm{A}} \quad {}_{22}^{\mathrm{A}}), \quad {}_2^{\mathrm{A}} \quad {}_{12}^{\mathrm{A}}\ {}_{31}^{\mathrm{A}} \quad {}_{32}^{\mathrm{A}}(c_1^{\mathrm{A}} \quad {}_{11}^{\mathrm{A}}), \\ {}_3^{\mathrm{A}} \quad (c_1^{\mathrm{A}} \quad {}_{11}^{\mathrm{A}})(c_2^{\mathrm{A}} \quad {}_{22}^{\mathrm{A}}) \quad {}_{12}^{\mathrm{A}}\ {}_{21}^{\mathrm{A}}, \quad {}^{\mathrm{A}} \quad \sqrt{({}_1^{\mathrm{A}})^2 \quad ({}_2^{\mathrm{A}})^2 \quad ({}_3^{\mathrm{A}})^2}. \end{gathered} \tag{14}$$

We should note that formulas (13) and (14) are of great importance in constructing a geometrically exact element of a composite shell under the action of a follower load, since they are employed in recalculating the external load at each step of the Newton–Raphson iteration process. It is precisely this factor that allows us to considerably reduce the number of loading steps.

Geometrically Exact Hybrid Bilinear Element of a Composite Shell

In [4, 6, 12], a family of geometrically exact bilinear 6-parameter shell elements based on the introduction of displacement-independent strains has been developed. Generalizing this method to the 7-parameter model and taking into account distribution (5), we can write

$$\overset{\mathrm{AS}}{\underset{\mathrm{A}}{}} N^{\mathrm{A}} E^{\mathrm{A}}, \quad \overset{\mathrm{AS}}{\underset{\mathrm{A}}{33}} N^{\mathrm{A}} E_{33}^{\mathrm{A}}, \quad \overset{\mathrm{AS}}{3} E_{3}, \tag{15}$$

where $E^{\mathrm{A}}(\ _1,\ _2)$, $E_{33}^{\mathrm{A}}(\ _1,\ _2)$, and $E_{3}(\ _1,\ _2)$ are the displacement-independent strains of external surfaces of the shell.

Since functional variables of different types are introduced in constructing a hybrid element, independent approximations must be used for them on each finite element [17]. For displacements, we employ the standard bilinear approximation

$$\mathbf{v} \quad \underset{r}{} N_r \mathbf{v}_r, \tag{16}$$

$$\mathbf{v} \quad [u_1\ u_2\ u_3\ u_1\ u_2\ u_3\ u_3^{\mathrm{M}}]^{\mathrm{T}}, \quad \mathbf{v}_r \quad [u_{1r}\ u_{2r}\ u_{3r}\ u_{1r}\ u_{2r}\ u_{3r}\ u_{3r}^{\mathrm{M}}]^{\mathrm{T}},$$

where $\mathbf{v}_r$ are the columns of nodal displacements; $N_r(\ _1,\ _2)$ are the bilinear shape functions; $(\quad d^{\mathrm{el}})/l^{\mathrm{el}}$ are the normalized curvilinear coordinates of the element; d^{el} are the center coordinates of the element; $2l^{\mathrm{el}}$ are the lengths of sides of the element. Hereinafter, $r \quad \overline{1,4}$.

For the independently introduced strains, we have even simpler approximations:

$$\mathbf{E} \quad \underset{r_1,r_2}{} (\ _1)^{r_1} (\ _2)^{r_2} \mathbf{Q}^{r_1 r_2} \mathbf{E}^{r_1 r_2},$$

$$\mathbf{E} \quad [E_{11}\ E_{11}\ E_{22}\ E_{22}\ E_{33}\ E_{33}\ 2E_{12}\ 2E_{12}\ 2E_{13}\ 2E_{23}]^{\mathrm{T}},$$

$$\mathbf{E}^{00} \quad [E_{11}^{00}\ E_{11}^{00}\ E_{22}^{00}\ E_{22}^{00}\ E_{33}^{00}\ E_{33}^{00}\ 2E_{12}^{00}\ 2E_{12}^{00}\ 2E_{13}^{00}\ 2E_{23}^{00}]^{\mathrm{T}}, \tag{17}$$

$$\mathbf{E}^{01} \quad [E_{11}^{01}\ E_{11}^{01}\ E_{33}^{01}\ E_{33}^{01}\ 2E_{13}^{01}]^{\mathrm{T}},$$

$$\mathbf{E}^{10} \quad [E_{22}^{10}\ E_{22}^{10}\ E_{33}^{10}\ E_{33}^{10}\ 2E_{23}^{10}]^{\mathrm{T}}, \quad \mathbf{E}^{11} \quad [E_{33}^{11}\ E_{33}^{11}]^{\mathrm{T}},$$

$$\mathbf{Q}^{01} \quad \begin{matrix} 1&0&0&0&0 \\ 0&1&0&0&0 \\ 0&0&0&0&0 \\ 0&0&0&0&0 \\ 0&0&1&0&0 \\ 0&0&0&1&0 \\ 0&0&0&0&0 \\ 0&0&0&0&0 \\ 0&0&0&0&1 \\ 0&0&0&0&0 \end{matrix}, \quad \mathbf{Q}^{10} \quad \begin{matrix} 0&0&0&0&0 \\ 0&0&0&0&0 \\ 1&0&0&0&0 \\ 0&1&0&0&0 \\ 0&0&1&0&0 \\ 0&0&0&1&0 \\ 0&0&0&0&0 \\ 0&0&0&0&0 \\ 0&0&0&0&0 \\ 0&0&0&0&1 \end{matrix}, \quad \mathbf{Q}^{11} \quad \begin{matrix} 0&0 \\ 0&0 \\ 0&0 \\ 0&0 \\ 1&0 \\ 0&1 \\ 0&0 \\ 0&0 \\ 0&0 \\ 0&0 \end{matrix},$$

where $\mathbf{Q}^{00}$ is the 10 10 unit matrix. Hereinafter, $r_1, r_2 = 0, 1$.

For the resulting pressures [9]

$$H^{\mathrm{A}} \quad \underset{k\ h_k}{} S^k\ N^{\mathrm{A}} d\ _3, \quad H_{33}^{\mathrm{A}} \quad \underset{k\ h_k}{} S_{33}^k N^{\mathrm{A}} d\ _3, \quad H\ _3 \quad \underset{k\ h_k}{} S^k{}_3 d\ _3 \tag{18}$$

we assume a similar approximation:

$$\mathbf{H} \quad \sum_{r_1,r_2} (\ _1)^{r_1} (\ _2)^{r_2} \mathbf{Q}^{r_1 r_2} \mathbf{H}^{r_1 r_2},$$

$$\mathbf{H} \quad [H_{11}\ H_{11}\ H_{22}\ H_{22}\ H_{33}\ H_{33}\ H_{12}\ H_{12}\ H_{13}\ H_{23}]^{\mathrm{T}},$$

$$\mathbf{H}^{00} \quad [H_{11}^{\ 00}\ H_{11}^{\ 00}\ H_{22}^{\ 00}\ H_{22}^{\ 00}\ H_{33}^{\ 00}\ H_{33}^{\ 00}\ H_{12}^{\ 00}\ H_{12}^{\ 00}\ H_{13}^{00}\ H_{23}^{00}]^{\mathrm{T}}, \tag{19}$$

$$\mathbf{H}^{01} \quad [H_{11}^{\ 01}\ H_{11}^{\ 01}\ H_{33}^{\ 01}\ H_{33}^{\ 01}\ H_{13}^{01}]^{\mathrm{T}},$$

$$\mathbf{H}^{10} \quad [H_{22}^{\ 10}\ H_{22}^{\ 10}\ H_{33}^{\ 10}\ H_{33}^{\ 10}\ H_{23}^{10}]^{\mathrm{T}}, \quad \mathbf{H}^{11} \quad [H_{33}^{\ 11}\ H_{33}^{\ 11}]^{\mathrm{T}},$$

where S_{ij}^{k} are components of the Piola–Kirchhoff symmetric strain tensor of a kth layer.

Introducing the distributions of (3), (5), and (15) and finite-element approximations (16), (17), and (19) into the Hu–Washizu mixed variational principle [18] and employing the standard procedure of the mixed FEM model, we derive the following equilibrium equations for the element:

$$\mathbf{E}^{r_1 r_2} \quad (\mathbf{Q}^{r_1 r_2})^{\mathrm{T}} (\mathbf{B}^{r_1 r_2} \quad \mathbf{R}^{r_1 r_2} \mathbf{V}) \mathbf{V}, \quad \mathbf{H}^{r_1 r_2} \quad (\mathbf{Q}^{r_1 r_2})^{\mathrm{T}} \mathbf{D} \mathbf{Q}^{r_1 r_2} \mathbf{E}^{r_1 r_2},$$

$$\sum_{r_1,r_2} \frac{1}{3^{r_1 \quad r_2}} (\mathbf{B}^{r_1 r_2} \quad 2\mathbf{R}^{r_1 r_2} \mathbf{V})^{\mathrm{T}} \mathbf{Q}^{r_1 r_2} \mathbf{H}^{r_1 r_2} \quad p^{\mathrm{A}} \mathbf{G}^{\mathrm{A}} (\mathbf{V}). \tag{20}$$

Here, $\mathbf{V} \quad [\mathbf{v}_1^{\mathrm{T}}\ \mathbf{v}_2^{\mathrm{T}}\ \mathbf{v}_3^{\mathrm{T}}\ \mathbf{v}_4^{\mathrm{T}}]^{\mathrm{T}}$ is the column of nodal displacements of an element of size 28 1; $\mathbf{B}^{r_1 r_2}$ are 10 28 matrices, *constant* inside the element, describing the linear components of Green–Lagrange strain tensor (6); $\mathbf{R}^{r_1 r_2}$ are three-dimensional 10 28 28 arrays, *constant* inside the element, describing the nonlinear components of the Green–Lagrange strain tensor (6) (in this case, $\mathbf{R}^{r_1 r_2} \mathbf{V}$ is a 10 28 matrix); p^{A} is the pressure distributed over one of the external surfaces $^{\mathrm{A}}$, and therefore the summation with respect to the A in the last equation of (20) is not required; $\mathbf{G}^{\mathrm{A}}(\mathbf{V})$ is a 28 1 column, which initially depends on the nodal values of the normal n_{ir}^{A} to the external surface of the deformed shell and finally, in view of relations (7), (13), (14), and (16) — on the nodal displacements u_{ir}^{A}; $\mathbf{D}$ is the matrix of elastic coefficients of the layered composite, whose elements are determined from the formulas

$$D_{ijlm}^{s_1 s_2} \quad \sum_{k \quad h_k} C_{ijlm}^{k} (N \quad)^{2 \quad s_1 \quad s_2} (N \quad)^{s_1 \quad s_2} d \quad _3 \quad (s_1, s_2 = 0, 1),$$

$$D \quad _3 \ _3 \quad D_{3 \ 3}^{00} \quad 2D_{3 \ 3}^{01} \quad D_{3 \ 3}^{11}, \tag{21}$$

where C_{ijlm}^{k} are the rigidities of a kth layer.

We should note that the system of equations (20) was derived on the assumption that the metrics of the external shell surfaces are equivalent to the metrics of the midsurface; an analytical integration [6-9], which is the prerogative of a geometrically exact shell element, was also performed.

To solve the nonlinear system (20), we will use an incremental approach. Let us consider two deformed (not necessarily close to each other) states of the shell and mark the quantities describing the previous state of the shell with a left superscript t and those belonging to the subsequent state with a left superscript t t, i.e.,

$$
\begin{gathered}
{}^{t\ \ t}p^{\mathrm{A}}\ {}^{t}p^{\mathrm{A}}\quad p^{\mathrm{A}},\quad {}^{t\ \ t}\mathbf{V}\ {}^{t}\mathbf{V}\quad \mathbf{V}, \\
{}^{t\ \ t}\mathbf{E}^{r_1r_2}\ {}^{t}\mathbf{E}^{r_1r_2}\quad \mathbf{E}^{r_1r_2},\quad {}^{t\ \ t}\mathbf{H}^{r_1r_2}\ {}^{t}\mathbf{H}^{r_1r_2}\quad \mathbf{H}^{r_1r_2},
\end{gathered}
\tag{22}
$$

where p^{A}, $\mathbf{V}$, $\mathbf{E}^{r_1r_2}$, and $\mathbf{H}^{r_1r_2}$ are incremental variables.

Inserting Eqs. (22) into Eqs. (20) and assuming that the latter are valid for an "instant of time" t, we come to an incremental form of the equilibrium equations for the finite element of the shell under the action of a follower pressure:

$$
\begin{gathered}
\mathbf{E}^{r_1r_2}\quad (\mathbf{Q}^{r_1r_2})^{\mathrm{T}}(\mathbf{B}^{r_1r_2}\quad 2\mathbf{R}^{r_1r_2}\,{}^{t}\mathbf{V}\quad \mathbf{R}^{r_1r_2}\quad \mathbf{V})\quad \mathbf{V}, \\
\mathbf{H}^{r_1r_2}\quad (\mathbf{Q}^{r_1r_2})^{\mathrm{T}}\,\mathbf{D}\mathbf{Q}^{r_1r_2}\quad \mathbf{E}^{r_1r_2}, \\
\frac{1}{\sum\limits_{r_1,r_2} 3^{r_1\ \ r_2}}\{2(\mathbf{R}^{r_1r_2}\quad \mathbf{V})^{\mathrm{T}}\mathbf{Q}^{r_1r_2}\,{}^{t}\mathbf{H}^{r_1r_2}\quad [\mathbf{B}^{r_1r_2}\quad 2\mathbf{R}^{r_1r_2}({}^{t}\mathbf{V}\quad \mathbf{V})]^{\mathrm{T}}\mathbf{Q}^{r_1r_2}\quad \mathbf{H}^{r_1r_2}\} \\
({}^{t}p^{\mathrm{A}}\quad p^{\mathrm{A}})\mathbf{G}^{\mathrm{A}}({}^{t}\mathbf{V}\quad \mathbf{V})\quad {}^{t}p^{\mathrm{A}}\mathbf{G}^{\mathrm{A}}({}^{t}\mathbf{V}).
\end{gathered}
\tag{23}
$$

The solution of incremental equations (23) is obtained according to the Newton–Raphson method by presenting the iterative process in the form

$$
\begin{gathered}
\mathbf{V}^{[n\ \ 1]}\quad \mathbf{V}^{[n]}\quad \hat{\mathbf{V}}^{[n]},\quad \mathbf{E}^{r_1r_2[n\ \ 1]}\quad \mathbf{E}^{r_1r_2[n]}\quad \hat{\mathbf{E}}^{r_1r_2[n]}, \\
\mathbf{H}^{r_1r_2[n\ \ 1]}\quad \mathbf{H}^{r_1r_2[n]}\quad \hat{\mathbf{H}}^{r_1r_2[n]}\quad (n = 0, 1,...).
\end{gathered}
\tag{24}
$$

Substituting relations (24) into Eqs. (23), linearizing the resulting equations, and excluding the incremental strains $\hat{\mathbf{E}}^{r_1r_2[n]}$ and the incremental resulting strains $\hat{\mathbf{H}}^{r_1r_2[n]}$, we come to the resolving FEM system of equations

$$
\mathbf{K}\ \ \hat{\mathbf{V}}^{[n]}\quad \mathbf{F}^{[n]}, \tag{25}
$$

where $\mathbf{K}\quad \mathbf{K}_{\mathrm{D}}\quad \mathbf{K}_{\mathrm{H}}\quad \mathbf{K}_{\mathrm{L}}$ is the tangential rigidity matrix of the shell element, and $\mathbf{F}^{[n]}$ is the column of the right-hand sides, which are calculated as

$$
\begin{gathered}
\mathbf{K}_{\mathrm{D}}\quad \frac{1}{\sum\limits_{r_1,r_2} 3^{r_1\ \ r_2}}({}^{t}\mathbf{L}^{r_1r_2[n]})^{\mathrm{T}}\,\mathbf{D}^{r_1r_2}\,{}^{t}\mathbf{L}^{r_1r_2[n]}, \\
\mathbf{K}_{\mathrm{H}}\quad 2\quad \frac{1}{\sum\limits_{r_1,r_2} 3^{r_1\ \ r_2}}(\mathbf{Q}^{r_1r_2}\,{}^{t}\mathbf{H}^{r_1r_2}\quad \mathbf{Q}^{r_1r_2}\quad \mathbf{H}^{r_1r_2[n]})\mathbf{R}^{r_1r_2}, \\
\mathbf{K}_{\mathrm{L}}\quad ({}^{t}p^{\mathrm{A}}\quad p^{\mathrm{A}})\frac{\mathbf{G}^{\mathrm{A}}}{\mathbf{V}}({}^{t}\mathbf{V}\quad \mathbf{V}^{[n]}),
\end{gathered}
\tag{26}
$$

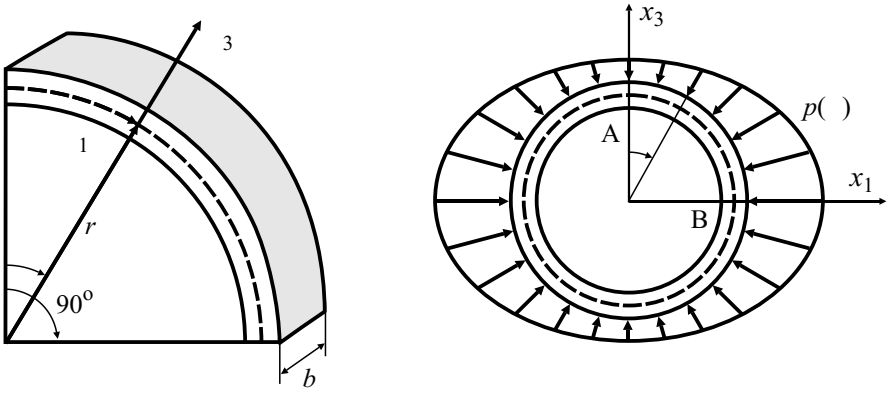

Fig. 2. A ring under the action of a follower load.

$$\mathbf{F}^{[n]} \quad \frac{1}{r_1, r_2 3^{r_1 \quad r_2}} [({}^t\mathbf{L}^{r_1 r_2 [n]})^{\mathrm{T}} \mathbf{D}^{r_1 r_2} ({}^t\mathbf{L}^{r_1 r_2 [n]} \quad \mathbf{R}^{r_1 r_2} \quad \mathbf{V}^{[n]})$$

$$2(\mathbf{Q}^{r_1 r_2} {}^t\mathbf{H}^{r_1 r_2}) \mathbf{R}^{r_1 r_2}] \quad \mathbf{V}^{[n]} \quad ({}^t p^{\mathrm{A}} \quad p^{\mathrm{A}}) \mathbf{G} \quad ({}^t\mathbf{V} \quad \mathbf{V}^{[n]}) \quad {}^t p^{\mathrm{A}} \mathbf{G} \quad ({}^t\mathbf{V}), \tag{26}$$

$${}^t\mathbf{L}^{r_1 r_2 [n]} \quad \mathbf{B}^{r_1 r_2} \quad 2\mathbf{R}^{r_1 r_2} ({}^t\mathbf{V} \quad \mathbf{V}^{[n]}), \quad \mathbf{D}^{r_1 r_2} \quad \mathbf{Q}^{r_1 r_2} (\mathbf{Q}^{r_1 r_2})^{\mathrm{T}} \mathbf{D} \mathbf{Q}^{r_1 r_2} (\mathbf{Q}^{r_1 r_2})^{\mathrm{T}}.$$

Note. The rigidity matrices $\mathbf{K}_{\mathrm{D}}$ and $\mathbf{K}_{\mathrm{H}}$ are *symmetric*. The symmetry of the second matrix can be revealed by using the results obtained in [9]. However, the rigidity matrix $\mathbf{K}_{\mathrm{L}}$, corresponding to the action of a follower load, is generally asymmetric [1, 19]; therefore, the solution of the system of linear algebraic equations (25), (26) is performed by the modified Gauss method for banded matrices [1]. We should also mention that the incremental resulting strains at an nth step of the iterative process are calculated by the formula

$$\mathbf{Q}^{r_1 r_2} \quad \mathbf{H}^{r_1 r_2 [n]} \quad \mathbf{D}^{r_1 r_2} \{[\mathbf{B}^{r_1 r_2} \quad 2\mathbf{R}^{r_1 r_2} ({}^t\mathbf{V} \quad \mathbf{V}^{[n \quad 1]})] \quad \mathbf{V}^{[n]}$$

$$(\mathbf{R}^{r_1 r_2} \quad \mathbf{V}^{[n \quad 1]}) \quad \mathbf{V}^{[n \quad 1]}\}, \quad \mathbf{V}^{[0]} \quad \mathbf{0}, \quad \mathbf{H}^{r_1 r_2 [0]} \quad \mathbf{0}, \quad n = 1, 2, \ldots .$$

The iterative process is continued until the fulfillment of the inequality

$$\left\| \mathbf{U}^{[n \quad 1]} \quad \mathbf{U}^{[n]} \right\| \quad \left\| \mathbf{U}^{[n]} \right\|, \tag{27}$$

where $\mathbf{U}$ is the global vector of nodal displacements, $\|\ldots\|$ is the Euclidean norm in the space of displacements, and is the calculation accuracy required, which is specified a priori.

Numerical Results

As a first example, we consider an isotropic ring (Fig. 2) ($E = 2.1 \ 10^7$ and $= 0.3$) and a two-layer composite ring ($E_{\mathrm{L}} \quad 2.5 \ 10^7, E_{\mathrm{T}} = 10^6, G_{\mathrm{LT}} = 5 \ 10^5, G_{\mathrm{TT}} = 2 \ 10^5$, and $_{\mathrm{LT}} \quad _{\mathrm{TT}} \quad 0.25$) under the action of a nonuniformly distributed follower pressure $p(\ ) \quad p_0 (1 \quad e\cos 2 \ )$. The geometrical parameters of both rings are $r = 100$, $h = 1$, and $b = 20$. The subscripts L and T correspond to the reinforcement and transverse directions of the composite material. The thickness of layers of the composite ring are assumed to be the same, i.e., $h_1 \quad h_2 \quad 0.5$, but the reinforcement directions in the internal and external layers coincide with the circumferential and longitudinal directions, respectively.

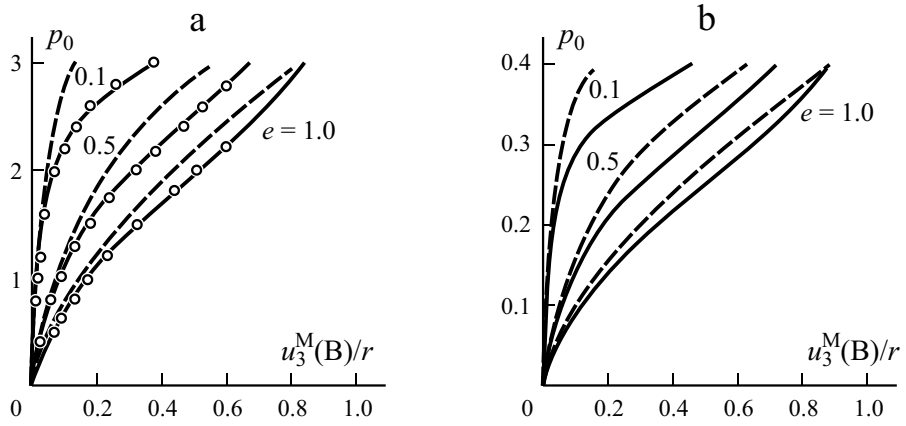

Fig. 3. Relations between the load and deflection $-u_3^{\mathrm{M}}$ with (——) and without (- - -) account of the follower load for the homogeneous (a) and the two-layer composite (b) rings. (○) — data [19] obtained by analytically solving the bending problem for an isotropic ring [20].

TABLE 1. Transverse Displacement $\bar{u}_3 \quad u_3^{\mathrm{M}} / r$ at the Points A and B of the Homogeneous Ring at $e = 1$ and $\bar{p}_0 = 3$

Element	NStep = 1			NStep = 5			NStep = 10		
	$\bar{u}_3$(A)	$\bar{u}_3$(B)	NIter	$\bar{u}_3$(A)	$\bar{u}_3$(B)	NIter	$\bar{u}_3$(A)	$\bar{u}_3$(B)	NIter
GEX7P4F	0.3660	0.8407	7	0.3660	0.8407	25	0.3660	0.8407	50
GEX7P4	0.3554	0.8220	6	0.3554	0.8220	18	0.3554	0.8220	30

TABLE 2. Transverse Displacement $\bar{u}_3 \quad u_3^{\mathrm{M}} / r$ at the Points A and B of the Two-Layer Composite Ring at $e = 1$ and $\bar{p}_0 = 0.4$

Element	NStep = 1			NStep = 5			NStep = 10		
	$\bar{u}_3$(A)	$\bar{u}_3$(B)	NIter	$\bar{u}_3$(A)	$\bar{u}_3$(B)	NIter	$\bar{u}_3$(A)	$\bar{u}_3$(B)	NIter
GEX7P4F	0.3647	0.8798	7	0.3647	0.8798	24	0.3647	0.8798	50
GEX7P4	0.3529	0.8831	6	0.3529	0.8831	18	0.3529	0.8831	30

Owing to symmetry of the problem, we consider only a quarter of the ring and use uniform 18 1 finite-element meshes. The calculations were carried out with the help of GEX7P4F and GEX7P4 geometrically exact bilinear shell elements developed with and without account of the follower load, which additionally allowed us to model a plane stress state. Figure 3 shows the load–deflection curves obtained at different values of the eccentricity *e*. As nondimensional load parameters, $\bar{p}_0 \quad 12 p_0 r^3 / E b h^3$ was chosen for the homogeneous ring and $\bar{p}_0 \quad 12 p_0 r^3 / E_{\mathrm{L}} b h^3$ for the composite one. The dots illustrate the data obtained in [19] by analytically solving the bending problem for an isotropic ring [20]. As is seen, the results of calculations with and without account of the follower pressure considerably differ at large deflections and small values of eccentricity. In Tables 1 and 2, the transverse displacement u_3^{M} at the points A and B obtained by using different numbers of load

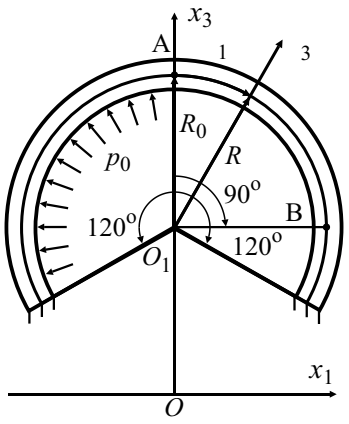

Fig. 4. Schematic sketch of a cross-ply rubber-cord toroidal shell.

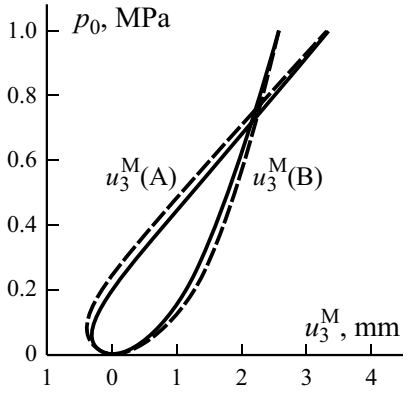

Fig. 5. Relations between the load p_0 and deflection u_3^M with (——) and without (- - -) account of the follower load for the rubber-cord toroidal shell.

TABLE 3. Transverse Displacement u_3^M (mm) at the Points A and B of the Cross-Ply Rubber-Cord Toroidal Shell at p_0 = 1 MPa

Element	NStep = 1			NStep = 5			NStep = 10		
	u_3^M (A)	u_3^M (B)	NIter	u_3^M (A)	u_3^M (B)	NIter	u_3^M (A)	u_3^M (B)	NIter
GEX7P4F	3.3409	2.5721	5	3.3409	2.5721	20	3.3409	2.5721	40
GEX7P4	3.3057	2.5649	5	3.3057	2.5649	16	3.3057	2.5649	31

steps, NStep, is presented, and the total number of iterations, NIter, necessary for achieving the specified accuracy $= 10^{-6}$ according to the criterion of convergence (27) is shown. We should mark off two important results: first, the solution of bending problems for isotropic and composite rings under the action of a follower pressure is possible without the use of the incremental approach (NStep = 1) and requires only seven iterations, and, second, the number of loading steps does not affect the calculated values of displacements, which confirms the efficiency of the geometrically exact shell elements constructed.

Now, let us consider a four-layer cross-ply rubber-cord toroidal shell of circular cross section, loaded with a pressure p_0 uniformly distributed over its inner surface (Fig. 4). This shell will be used for modeling a diagonal tire. The initial characteristics of the elementary rubber-cord layers are [21] $E_{\mathrm{L}} = 510.45$ MPa, $E_{\mathrm{T}} = 6.91$ MPa, $G_{\mathrm{LT}} = 2.33$ MPa, $G_{\mathrm{TT}} = 1.77$ MPa, and $_{\mathrm{LT}} = 0.46$. Let the shell thickness be $h = 4.8$ mm, the thickness of a rubber-cord layer $h_k = 1.2$ mm, and the orientations of rubber-cord layers $_k$ ($1)^{k\ 1}$, where $= 45$ and k $\overline{1, 4}$. As a reference surface, we assume the shell midsurface formed by rotation of a part of the circumference of radius $R = 50$ mm. The distance from the rotation axis to the equator of midsurface R_0 250 mm; the cross sections of the shell with the coordinates 120 are rigidly clamped.

Calculation results for the tire under the action of follower and conservative loads were obtained by using regular 24 1 finite-element meshes at $= 10^{-6}$ (see Table 3 and Fig. 5). As is seen, the data in Tables 1 and 3 agree in a qualitative sense with each other. In particular, the solution of this problem for a diagonal tire can also be found without using the incremental approach. However, here the influence of the follower load does not appear so noticeably (see Figs. 3 and 5).

In the following investigation, the present authors are going to generalize the results obtained and use them for calculating a rubber-cord shell of revolution in the presence of unilateral restrictions.

This study was financially supported by the Russian Fund for Basic Research (Project No. 08-01-00373) and the Ministry of Education of Russian Federation (Project № 2.1.1/660).

REFERENCES

1. O. C. Zienkiewicz and R. L. Taylor, The Finite Element Method. Vol. 2. Solid Mechanics, Butterworth Heinemann, Oxford (2000).
2. L. O. Faria, J. T. Oden, B. Yavary, W. W. Tworzydlo, J. M. Bass, and E. B. Becker, "Tire modeling by finite elements," Tire Sci. Technol., **20**, No 1, 33-56 (1992).
3. K. T. Danielson, A. K. Noor, and J. S. Green, "Computational strategies for tire modeling and analysis," Comput. Struct., **61**, No. 4, 673-693 (1996).
4. G. M. Kulikov and S. V. Plotnikova, "Investigation of locally loaded multilayer shells by a mixed finite-element method. 1. Geometrically nonlinear statement," Mech. Compos. Mater., **38**, No. 6, 539-546 (2002).
5. G. M. Kulikov, "Deformation relations exactly representing large rigid-body displacements of shells," Mekh. Tverd. Tela, **39**, No. 5, 130-140 (2004).
6. G. M. Kulikov and S. V. Plotnikova, "Non-linear strain–displacement equations exactly representing large rigid-body motions. Part II. Enhanced finite element technique," Comput. Meth. Appl. Mech. Eng., **195**, Nos. 19-22, 2209-2230 (2006).
7. G. M. Kulikov and S. V. Plotnikova, "Geometrically exact assumed stress-strain multilayered solid-shell elements based on the 3D analytical integration," Comput. Struct., **84**, Nos. 19-20, 1275-1287 (2006).
8. G. M. Kulikov and S. V. Plotnikova, "Non-linear strain-displacement equations exactly representing large rigid-body motions. Part III. Analysis of TM shells with constraints," Comput. Meth. Appl. Mech. Eng., **196**, No. 7, 1203-1215 (2007).
9. G. M. Kulikov and S. V. Plotnikova, "Finite rotation geometrically exact four-node solid-shell element with seven displacement degrees of freedom," Comput. Model. Eng. Sci., **28**, No. 1, 15-38 (2008).
10. E. I. Grigolyuk and G. M. Kulikov, "Axisymmetric deformation of anisotropic multilayer shells of revolution of intricate shapes," Mech. Compos. Mater., **17,** No. 4, 437-445 (1981).
11. H. Y. Roh and M. Cho, "The application of geometrically exact shell elements to B-spline surfaces," Comput. Meth. Appl. Mech. Eng., **193**, Nos. 23-26, 2261-2299 (2004).
12. G. M. Kulikov and S. V. Plotnikova, "Non-linear geometrically exact assumed stress-strain four-node solid-shell element with high coarse-mesh accuracy," Finite Elem. Anal. Des., **43**, Nos. 6-7, 425-443 (2007).
13. H. Parisch, "A continuum-based shell theory for non-linear applications," Int. J. Numer. Meth. Eng., **38**, No. 11, 1855-1883 (1995).

14. M. Bischoff, W. A. Wall, K. U. Bletzinger, and E. Ramm, “Models and finite elements for thin-walled structures,” in: E. Stein, R. de Borst, T. J. R. Hughes (eds.), Encyclopedia of Computational Mechanics. Vol. 2. Solids and Structures, Willey (2004), pp. 59-137.
15. G. M. Kulikov, “Refined global approximation theory of multilayered plates and shells,” J. Eng. Mech., **127**, No. 2, 119-125 (2001).
16. A. L. Gol’denveyzer, Theory of Elastic Thin Shells [in Russian], Nauka, Moscow (1976).
17. T. H. H. Pian, “State-of-the-art development of hybrid/mixed finite element method,” Finite Elem. Anal. Des., **21**, No. 1, 5-20 (1995).
18. K. Washizu, Variational Methods in Elasticity and Plasticity, Pergamon Press, Oxford (1975).
19. J. H. Argyris and S. Symeonidis, “Nonlinear finite element analysis of elastic systems under nonconservative loading — natural formulation. Part I. Quasistatic problems,” Comput. Meth. Appl. Mech. Eng., **26**, No. 1, 75-123 (1981).
20. P. Seide and T. M. M. Jamjoom, “Large deformations of circular rings under nonuniform normal pressure,” J. Appl. Mech., **41**, No. 1, 192-196 (1974).
21. G. M. Kulikov, “Computational models for multilayered composite shells with application to tires,” Tire Sci. Technol., **24**, No. 1, 11-38 (1996).